European Review for Medical and Pharmacological Sciences 2020; 24: 6455-6462

Hydroxytyrosol suppresses LPS-induced intrahepatic inflammatory responses *via* inhibition of ERK signaling pathway activation in acute liver injury

Y.-B. YU, H.-Z. ZHUANG, X.-J. JI, L. DONG, M.-L. DUAN

Intensive Care Unit, Beijing Friendship Hospital, Capital Medical University, Beijing, China

Abstract. – OBJECTIVE: Acute liver injury (ALI) leads to inflammatory response and tissue damage. Inflammatory activation of infiltrative macrophages plays a critical role in liver histology destruction and dysfunction. Hydroxytyrosol (3,4-dihydroxyphenil-ethanol, HT), one of the polyphenols extracted from extra virgin olive oil, currently acts as a treatment for neuroinflammatory responses, but its effect on ALI is elusive. The present study aims to examine the mechanism of HT in macrophages inflammation and evaluate treatment effect of HT on ALI.

MATERIALS AND METHODS: *In vitro*, the expressions of type M1/M2 macrophages biomarkers (CD11c/CD206) and cytokines (TNF-α, IL-1β, IL-6, IL-10, IL-4) following lipopolysaccharide (LPS) stimulation and HT administration were detected using immunofluorescence, quantitative real-time polymerase chain reaction (qRT-PCR), and enzyme-linked immunosorbent assay (ELISA). Mechanically, HT was used to treat cells and phosphorylation level of extracellular-signal-regulated kinase 1/2 (ERK1/2) protein in cells was analyzed using Western blotting. In murine acute liver injury, inflammatory cytokines and liver injury degree were exhibited by qRT-PCR, IHC and HE staining. Furthermore, hepatic function was exhibited *via* hepatic metabolic enzymes (ALT/AST) and total bilirubin (TBil) in serum.

RESULTS: It was demonstrated that HT treatment attenuated M1 macrophages and increased M2 macrophages after LPS stimulation. Furthermore, the pro-inflammatory cytokine level was descended, while an-inflammatory cytokine was increased *via* HT suppressing ERK pathway in macrophages. *In vivo*, HT reduced inflammatory level and mitigated hepatic histological injury, thus ameliorating liver function after acute liver injury.

CONCLUSIONS: HT exerts a hepatoprotective and anti-inflammation effect on acute liver injury, which restrains inflammation by inhibiting ERK pathway and regulating macrophages polarization. Moreover, HT prevents liver tissues from inflammatory injury. Therefore, HT serves as a potential implication to treat ALI through modulating inflammation of macrophages.

Key Words:
Hydroxytyrosol, Macrophages, Inflammation, ERK pathway, Acute liver injury.

Introduction

Acute liver injury (ALI) a destructive disease that results in histological damage and disorders of metabolomics[1,2]. ALI can be elicited by multiple inducements including intemperance, drug abuse, virus infection and immunologic process[3-5]. Although the pathogenesis of ALI has been widely explored, therapeutic methods of alleviating ALI remain uncertain. Hepatocyte injury and death resulting from granulocytes infiltration are features of the injured liver, which may aggravate structural destruction, metabolic hypofunction and even trigger acute liver failure. Tsutsui et al[6] confirmed that negative modulation of inflammatory level in ALI could attenuate hepatic parenchymal injury, indicating that the reverse of excessive inflammation at early stage may control the aggravation of ALI. Inflammation, serving as a pathological immunologic process[7], is involved in tissue injury process when over-expressed, which contributes to overwhelming leukocytes into liver tissue and a mass of pro-inflammatory cytokines to exacerbate histological destruction and ultimately inducing hepatocytes apoptosis. To control inflammation process and decrease liver injury area, regulating macrophages bioactivity is a significant therapy direction. Macrophages are a kind of bone marrow-derived monocytes and possess phagocytic

Corresponding Author: Meili Duan, MD; e-mail: yyyyjycyu@126.com

and polarization ability in congenital and cellular immunity, which perform phagocytic function in fragments and pathogens[8]. There are two types of macrophages, namely M1 considered to be pro-inflammation phenotype and M2 characterized as anti-inflammation. Over-activated M1 macrophages in lesion proliferate and secrete toxic nitric oxide *via* consuming the substrate arginine to induce secondary injury and enlarge injured area[9]. However, M2 macrophages activation releases multiple anti-inflammation factors and promotes tissue remodeling[10]. The polarization of macrophages in pro-inflammation or anti-inflammation type is critical to histologic lesion and repair[11,12]. Hence, recent researches have been concentrating on the understanding of macrophages differentiation regulation in an expectation that advanced treatment controls inflammation progression. Hydroxytyrosol (3,4-dihydroxyphenil-ethanol, HT), a small-molecule compound isolated from olive oil[13], modulates oxidative stress, inflammation and thrombogenesis. HT plays a protective role in liver steatosis diseases[14-16]. Particularly, HT modulates neuroinflammatory in lipopolysaccharide (LPS)-induced microglia *via* suppression of toll like receptor-4 (TLR-4)-mediated nuclear factor-κB (NF-κB) P65 activation[17]. But HT's effects on ALI have not been reported and the mechanism of HT on macrophages in ALI is unclear. It has been recognized that HT may change pathogenetic process of ALI through modulating macrophage polarization. In this study, HT was hypothesized to mediate related pathway of macrophages and reduce inflammatory factors and increase anti-inflammatory factors expressions. To testify the hypothesis, HT in macrophage line RAW 264.7 cells was utilized, and the effect and mechanism of HT on inflammation regulation in LPS-induced macrophages and ALI were explored.

Materials and Methods

Cell Culture and Treatment

Macrophage RAW 264.7 cells were obtained from American Type Culture Collection (ATCC) (Manassas, VA, USA). Primary cells were digested with 0.25% trypsin (Gibco, Rockville, MD, USA) inoculated in a 25 cm^2 cell flask with Dulbecco's Modified Eagle's Medium (DMEM, KeyGEN, Nanjing, China) containing 10% fetal bovine serum (FBS, Gibco, Rockville, MD, USA)/1% penicillin-streptomycin. When RAW 264.7 cells grew to 100% confluence, they were transferred into a 6-well plate. After starvation treatment with free serum DMEM for 24 h, HT (50 or 100 μM) was utilized to pretreat RAW 264.7 cells for 12 h, and then lipopolysaccharide (LPS, 100 ng/mL, Sigma-Aldrich, St. Louis, MO, USA) were employed to activate RAW 264.7 cells for 24 h.

Mice and ALI Model

Male C57BL/6 mice (6-8W) were purchased from Capital Medical University Animal Center and housed in Capital Medical University Animal Center. This investigation was approved by the Animal Ethics Committee of Capital Medical University Animal Center. In this study, mice were randomly assigned into three groups (control, LPS, and HT + LPS group) and littermates were ear tagged. LPS solution prepared with 0.9% normal saline (10 mg/kg, i.p.) was used to treat mice to induct ALI in mice. Then, HT (100 mg/kg, po., q.d, daily for 2 days) was performed to medication. Only HT injection was administrated in ALI+ dasatinib group. Mice were anesthetized with ketamine/xylazine and perfused with phosphate-buffered saline (PBS) for RNA isolation or 4% paraformaldehyde (PFA) for immunostaining.

Quantitative Reverse Transcription-Polymerase Chain Reaction (qRT-PCR)

Total RNA was extracted from RAW 264.7 cells and liver tissue homogenate using a TRIzol reagent (Beyotime Biotechnology, Shanghai, China) according to the manufacturer's protocol. 1 μg of RNA was reversely transcribed to complementary deoxyribose nucleic acid (cDNA) using RevertAid First strand cDNA synthesis kit (Thermo Fisher Scientific, Waltham, MA, USA). Quantification of the RNAs was performed using SYBR Green qPCR Mater Mix (Thermo Fisher Scientific, Waltham, MA, USA). Thereafter, melting curve analysis was used to determination of every reaction specificity. Glyceraldehyde 3-phosphate dehydrogenase (GAPDH) was used for normalization and all reactions were repeated in triplicate using a real-time PCR system. Finally, the relative mRNA expression was quantified by the $2^{-\Delta\Delta Ct}$ methods. Full list of primers used is provided as follows. TNF-α, Forward Primer, CAGGCGGTGCCTATGTCTC; Reverse Primer, CGATCACCCCGAAGTTCAGTAG. IL-1β, Forward Primer, TTCAGGCAGGCAGTATCACTC; Reverse Primer, GAAGGTCCACGGGAAAGACAC. IL-6, Forward Primer, CTGCAAGAGACTTCCATC-

CAG; Reverse Primer, AGTGGTATAGACAG-GTCTGTTGG. IL-10, Forward Primer, CT-TACTGACTGGCATGAGGATCA and Reverse Primer, GCAGCTCTAGGAGCATGTGG. IL-4, Forward Primer, GGTCTCAACCCCCAGCTAGT and Reverse Primer, GCCGATGATCTCTCT-CAAGTGAT. GAPDH, Forward Primer, TGG-CCTTCCGTGTTCCTAC and Reverse Primer, GAGTTGCTGTTGAAGTCGCA.

Western Blot (WB) Analysis

Cells were harvested in lysis buffer supplemented phenylmethylsulfonyl fluoride (PMSF) and phosphatase inhibitors/ proteinase inhibitor then total proteins were extracted. Proteins concentration was detected using an enhanced bicinchoninic acid (BCA) Protein Assay Kit (Beyotime, Shanghai, China). Next, electrophoretic separation, transferring and blocking were conducted. Then, proteins were incubated with anti-COX-2 (Abcam, Cambridge, MA, USA, 1:1000), anti-ERK1/2 (Abcam, Cambridge, MA, USA, 1:1000), anti-p-ERK1/2 (Abcam, Cambridge, MA, USA, 1:1000) and anti-GAPDH (CST, Danvers, MA, USA, 1:2000) overnight. After washed with Tris- Buffered Saline and Tween-20 (TBST) for 10 min, the proteins were incubated with secondary antibody (YiFeiXue, Nanjing, China, 1:5000) for 1 h at room temperature. At last, the proteins were visualized using an enhanced chemiluminescence (ECL) system.

Immunofluorescence (IF)

RAW 264.7 cells in 12-well plate were fixed with 4% PFA for 15 min and blocked for 1 h. Washed with PBS, cells were incubated with CD11c (Abcam, Cambridge, MA, USA, 1:100) and CD206 (Abcam, Cambridge, MA, USA, 1:200) overnight at 4°C. Then, the cells were washed by PBS and combined with an Alexa Fluor 488 or 594-conjugated AffiniPure F(ab')2 Fragment Goat Anti-Rabbit IgG (H+L) (Jackson, West Grove, PA, USA, 1:500) for 1 h at room temperature. After that, nucleus counterstaining and mounting were conducted using a 4',6-diamidino-2-phenylindole (DAPI)-Fluoromount-G (Southern Biotech, Birmingham, AL, USA). Finally, images were collected using a fluorescence microscope.

Immunohistochemical and Hematein Eosin Staining

Hepatic tissue was fixated with 4% PFA and received dehydration through different gradients of alcohol. Then, samples were embedded into paraffin and cut into sections (5 μm) using a rotary microtome. Hematoxylin-eosin (HE) staining was conducted using a Hematoxylin and Eosin Staining Kit (Beyotime, Shanghai, China). Hepatic sections were incubated with CD11c (Abcam, Cambridge, MA, USA, 1:100), COX-2 (Abcam, Cambridge, MA, USA, 1:200) CD206 (Abcam, Cambridge, MA, USA, 1:100). Thereafter, IHC staining was conducted using Rabbit&Mouse HRP Kit (DAB, WE0316-JKS, Biolab, Madrid, Spain) following manufacturer's instruction. Then, the images of sections were visualized and collected using a microscope.

Enzyme-Linked Immunosorbent Assay (ELISA)

Serum was taken from mice, collected and centrifuged for 10 min, and then their supernatant was collected. ELISA detection was conducted using an ELISA Kit (MultiSciences, Hangzhou, China). Standard products and samples in each group were successively added into a 96-well plate. Then, the colorant was seeded into each well and the plate was placed in the dark for 15 min. Finally, the reaction was terminated using the terminal, and the absorbance (OD value) of each well was measured at 450 nm.

Statistical Analysis

Data were exhibited as the means ± SD (standard deviations). Differences between two groups were analyzed by using the Student's *t*-test. Comparison between multiple groups was done using One-way ANOVA test followed by Post-Hoc Test (Least Significant Difference). Data were collected and analyzed using Statistical Product and Service Solutions (SPSS) 16.0 software (SPSS Inc., Chicago, IL, USA). When $p<0.05$, the difference was statistically significant.

Results

HT Inhibits Pro-Inflammatory Factors and Reduces Inflammatory Expression in RAW 264.7 Cells

First, to verify whether HT inhibits inflammation in RAW 264.7 cells, cyclooxygenase-2 (COX-2) expression following LPS stimuli and HT treatment was examined. Western blotting exhibited that LPS significantly increased COX-2 expression while HT reduced COX-2 level after LPS stimulation with a concentration gradient (Figure

1A). Further, the RNA levels of tumor necrosis factor-alpha (TNF-α), interleukin-1 beta (IL-1β) and interleukin-6 (IL-6) were detected, finding that TNF-α, IL-1β and IL-6 were decreased in RNA level after HT treatment (Figure 1B-1D). TNF-α, IL-1β and IL-6 expressions were also measured using ELISA, showing that LPS remarkably enhanced TNF-α, IL-1β and IL-6 expressions in cells. However, 50 μM and 100 μM HT administration reversed the above inflammatory cytokines expression after LPS activation in cells (Figure 1E-1G). Hence, HT inhibits pro-inflammatory factors and alleviates inflammatory level.

Administration of HT Promotes Macrophages M2 Polarization Via Regulation of ERK Signaling

To explore the mechanism of HT concerning anti-inflammatory effect on the RAW 264.7 cells, LPS and 100 μM of HT were further employed to treat the RAW 264.7 cells, and the polarization levels of M1 and M2 were measured using IF staining. It was found that M1 cells (CD11c positive) were increased after LPS utilization while M2 cells (CD206 positive) were at low expression, but HT treatment remarkably elevated M2 cell polarization following LPS stimulation (Figure 2A). Besides, the RNA levels of IL-10 and IL-4 were measured, exhibiting that HT increased IL-10 and IL-4 expressions after LPS treatment (Figure 2B, 2C). Besides, the phosphorylation level of ERK1/2 in the LPS-activated RAW 264.7 cells was detected. WB showed that p-ERK1/2 was increased remarkably in LPS group. However, HT decreased p-ERK1/2 but they all did not affect the ERK1/2 expression (Figure 2D). Thereof, the results indicate that HT promotes macrophages M2 polarization and increases anti-inflammatory cytokines through restraining ERK1/2 pathway.

HT Treatment Reduces Intrahepatic Inflammation Level and Alleviates Liver Tissue Injury

In vivo, ALI mice were treated with HT or not. IHC staining displayed that CD11c and COX-2 expressions in ALI group were remarkably higher than those in control group, but HT treatment effectively inhibited CD11c and COX-2 levels in injured liver (Figure 3A). Moreover, the RNA levels of pro-inflammatory cytokines (TNF-α, IL-1β and IL-6) in liver tissue were measured using qRT-PCR, exhibiting that HT could negatively modulate the RNA levels of TNF-α, IL-1β and IL-6 after ALI (Figure 3B-3D). Besides, the injury degree of liver

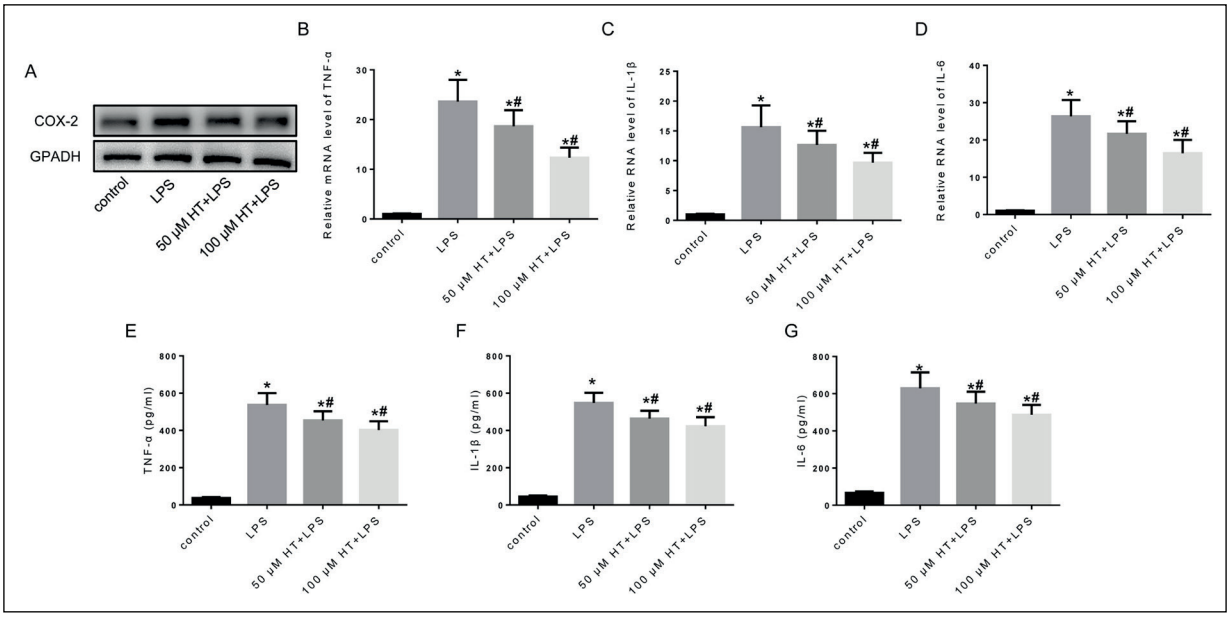

Figure 1. HT inhibits pro-inflammatory factors and reduces inflammatory expression in RAW 264.7 cells. **A,** Representative COX-2 level in control, LPS, 50 μM HT+LPS and 100 μM HT+LPS group. **B-D,** Quantitative RNA levels of TNF-α, IL-1β and IL-6 in control, LPS, 50 μM HT+LPS and 100 μM HT+LPS group. **E-G,** Representative ELISA of TNF-α, IL-1β and IL-6 in control, LPS, 50 μM HT+LPS and 100 μM HT+LPS group. "*" means *vs.* control group, "#" means *vs.* LPS group with statistical significance.

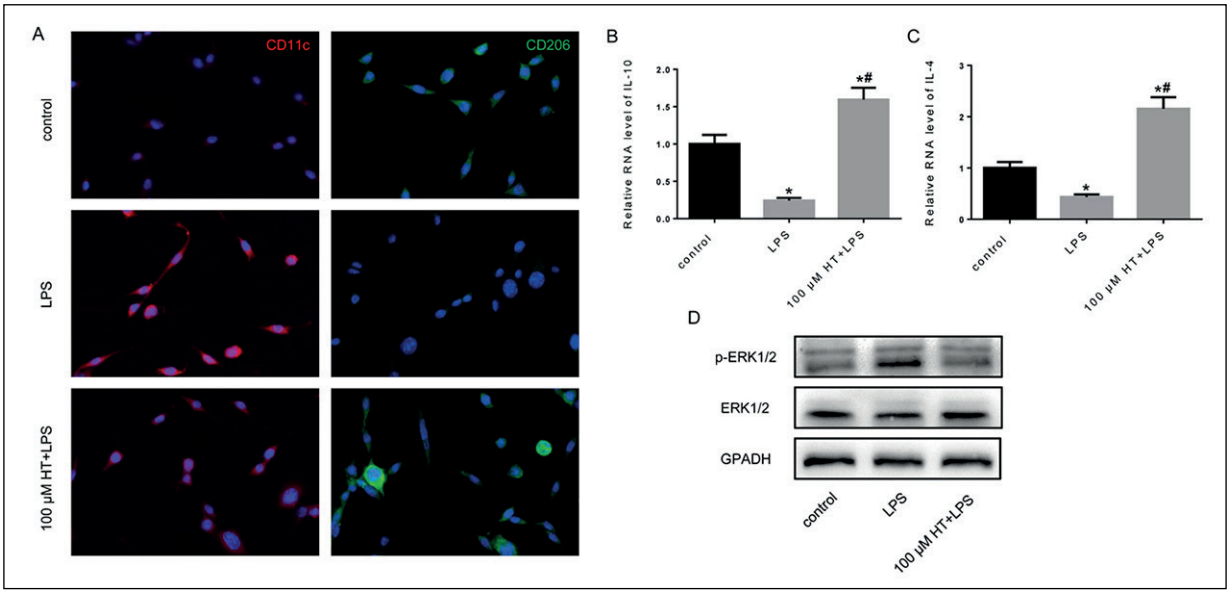

Figure 2. Administration of HT promotes macrophages M2 polarization *via* regulation of ERK signaling. **A,** Representative IF staining of CD11c (red) and CD206 (green) in control, LPS and 100 μM HT+LPS group (magnification: 400×). **B-C,** Quantitative RNA levels of IL-10 and IL-4 in control, LPS and 100 μM HT+LPS group. **D,** Representative Western blotting of p-ERK1/2 and ERK1/2 in control, LPS and 100 μM HT+LPS group. "*" means *vs.* control group, "#" means *vs.* LPS group with statistical significance.

was reflected using HE staining. The images displayed that HT administration reduced infiltration, tissue edema and vacuolation in liver. Hence, it can be concluded that HT reduces intrahepatic inflammation level and alleviates tissue injury after ALI (Figure 3E).

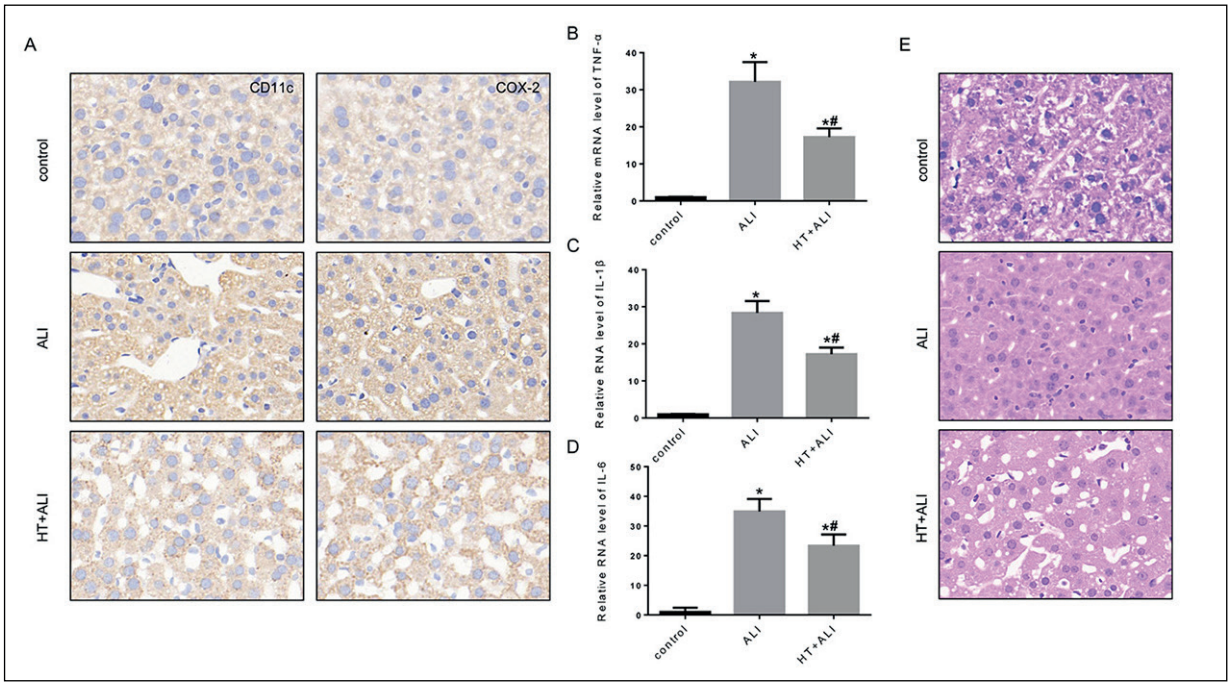

Figure 3. HT treatment reduces intrahepatic inflammation level and alleviates liver tissue injury. **A,** Representative IHC staining of CD11c and COX-2 in control, ALI, and HT+ALI group (magnification: 400×). **B-D** Representative RNA levels of TNF-α, IL-1β and IL-6 in control, ALI, and HT+ALI group. **E,** Representative HE staining of liver tissue in control, ALI, and HT+ALI group. (magnification: 400×) "*" means *vs.* control group with statistical significance. "#" means *vs.* ALI group with statistical significance.

HT Promotes Anti-Inflammatory Macrophages Expression and Protects Liver Function After ALI

The serum of mice was collected, and IL-10 and IL-4 in each group were detected using ELISA, showing that HT significantly increased IL-10 and IL-4 in serum (Figure 4A, 4B). IHC also exhibited that HT treatment elevated CD206 expression in liver tissues (Figure 4C). Besides, serum glutamic-pyruvic aminotransferase (ALT), glutamic oxalacetic aminotransferase (AST) and total bilirubin (TBil) were examined to evaluate liver function. The results exhibited that excessive ALT and AST were increased in consistent with elevated TBil in serum after ALI, but HT administration restrained the elevation of ALT, AST and TBil in serum (Figure 4D, 4E), indicating that HT protects liver function following ALI.

Discussion

Macrophage polarization is a critical process participating in pathogenic inflammation response. M1 macrophages promote inflammatory cascades in injured tissues and induct distensible lesions, while M2 macrophages release multiple anti-inflammation factors and phagocytose cell fragments and pathogens. In ALI, excessive and continuous inflammation could cause organic dysfunction and even hepatic failure, which provokes accumulating inflammatory mediators and initiates apoptosis procedure in tissues[18]. Regulating M1 cells to M2 cells in liver at early stage can mitigate secondary injury and conserve liver function[19-21]. Thereof, the directed transition of macrophages after liver injury was researched to explore a valid therapy. HT is an important constituent of the Mediterranean diet. Of note, Silva et al[22] reported the protective effect of HT on rheumatoid arthritis *via* inhibiting acute inflammation. Considering the above, it was assumed that HT may attenuate inflammation of macrophages in ALI and take a protective effect on liver tissue. Herein, it was firstly found that HT down-regulated COX-2 expression and several typical pro-inflammatory cytokines in the RAW 264.7 cells following LPS stimulation. To verify this, whether HT regulates RAW 264.7 cell phenotype *in vitro* was next investigated. Zhang et

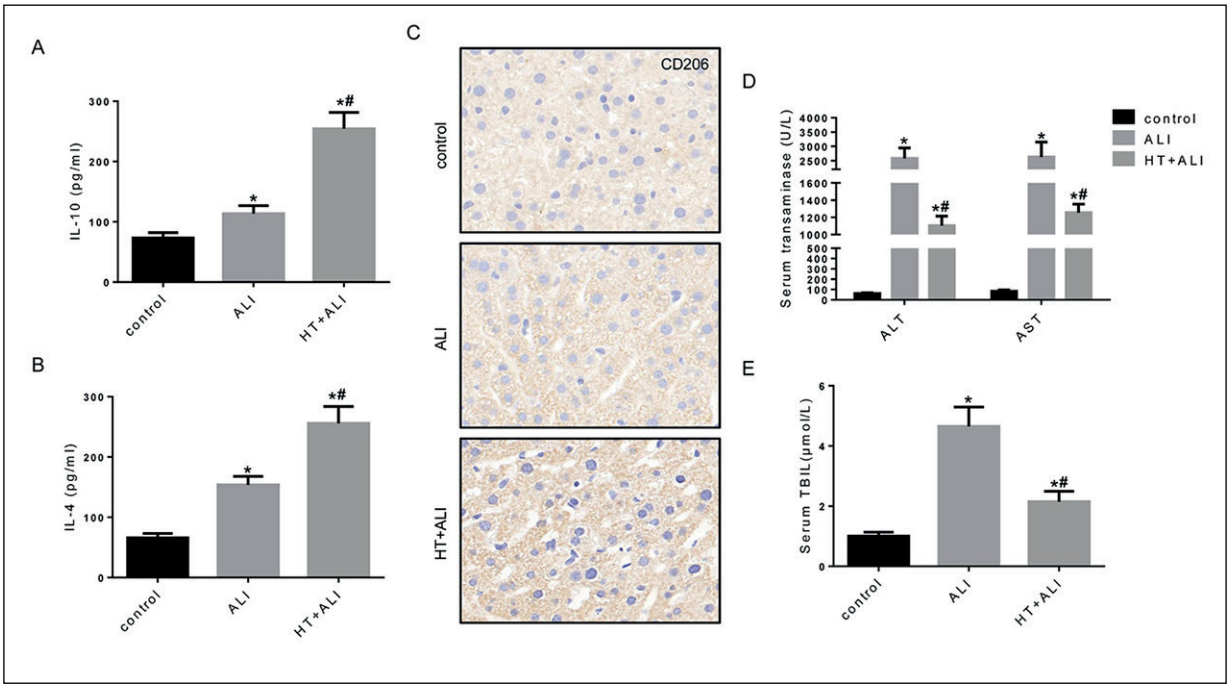

Figure 4. HT promotes anti-inflammatory macrophage expression and protects liver function after ALI. **A-B,** Representative ELISA of IL-10 and IL-4 in control, ALI, and HT+ALI group. **C,** Representative IHC staining of CD206 in control, ALI, and HT+ALI group (magnification: 400×). **D-E,** Representative serum aminotransferase and TBil in control, ALI, and HT+ALI group. "*" means *vs.* control group with statistical significance. "#" means *vs.* ALI group with statistical significance.

al[17] showed that HT alleviates neuroinflammation in microglia through reducing M1 cells expression and increasing M2 cell expression, so the M1 marker CD11c and M2 marker CD206 in LPS-activated RAW 264.7 cells were detected, showing that HT treatment led to visible decreased expression of CD11c and increased CD206 expression. The result further proved that HT displayed an anti-inflammatory effect on macrophage line polarization. Mechanically, ERK1/2 pathway is a critical regulatory signaling pathway in macrophage phenotype. In LPS-induced inflammation, the activation of ERK1/2 pathway in macrophages could induce inflammatory M1 polarization. Hence, it was suspected that HT serving as a potent anti-inflammatory agent may alleviate inflammatory response *via* inhibiting ERK1/2 pathway activation in macrophages. It was observed that HT showed apparent downregulation of phosphorylated ERK1/2 protein in LPS-activated RAW 264.7 cells, indicating that HT may exert anti-inflammatory effect *via* inhibiting ERK1/2 pathway. Also, to further demonstrate the efficacy of HT on hepatic inflammation and hepatic histology after ALI, inflammation level and injured degree in liver were assessed. LPS injection in murine evokes acute injury to liver tissues and then oral HT was employed in mice. Inflammatory M1 macrophages are associated with progressive inflammation and intrahepatic injury following ALI, but the M2 phenotype of anti-inflammation can improve hepatic functional and histological integrity. In ALI mice, it was exhibited that HT negatively modulated intrahepatic inflammation after ALI *via* decreasing M1 type and increasing M2 type. Besides, the RNA levels of TNF-α, IL-1β and IL-6 declined and the release of IL-10 and IL-4 increased in serum following HT treatment. Briefly, the above results in our study supported the view that HT ameliorated intrahepatic inflammation and improved liver tissues and functions through modulating direction of macrophages polarization. Terminally, due to the restriction of the M1 macrophages and promotion of M2 macrophages in liver with HT treatment, hepatic impairment in histology and function were eventually mitigated. All the data indicate that HT may be a promising hepatoprotective effect and anti-inflammatory drug by targeting macrophages phenotype. The novelties of the study are that the improved effect of HT on ALI via targeting macrophage polarization was firstly presented, and the anti-inflammatory role of HT through modulating ERK1/2 pathway in macrophage was illuminated, but pharmacokinetics and other aspects of liver protection will remain to be explored deeply.

Conclusions

Altogether, the above results suggest that HT treatment mitigates ALI in mice through reverse polarizing M1 macrophages to M2 macrophages, resulting in decreased inflammatory cytokines and increased anti-inflammatory cytokines. HT also attenuates hepatic histological and functional impairment following ALI, so HT may be a promising compound to treat ALI.

Conflict of Interest

The Authors declare that they have no conflict of interests.

Funding Acknowledgements

Stratified diagnosis and treatment of acute severe infection (ZYLX201802).

References

1) Gonzalez E, van Liempd S, Conde-Vancells J, Gutierrez-de JV, Perez-Cormenzana M, Mayo R, Berisa A, Alonso C, Marquez CA, Barr J, Lu SC, Mato JM, Falcon-Perez JM. Serum UPLC-MS/MS metabolic profiling in an experimental model for acute-liver injury reveals potential biomarkers for hepatotoxicity. Metabolomics 2012; 8: 997-1011.
2) Wree A, Dechene A, Herzer K, Hilgard P, Syn WK, Gerken G, Canbay A. Steroid and ursodesoxycholic Acid combination therapy in severe drug-induced liver injury. Digestion 2011; 84: 54-59.
3) Russo MW, Galanko JA, Shrestha R, Fried MW, Watkins P. Liver transplantation for acute liver failure from drug induced liver injury in the United States. Liver Transpl 2004; 10: 1018-1023.
4) Gujral JS, Farhood A, Bajt ML, Jaeschke H. Neutrophils aggravate acute liver injury during obstructive cholestasis in bile duct-ligated mice. Hepatology 2003; 38: 355-363.
5) Ishida Y, Kondo T, Ohshima T, Fujiwara H, Iwakura Y, Mukaida N. A pivotal involvement of IFN-gamma in the pathogenesis of acetaminophen-induced acute liver injury. FASEB J 2002; 16: 1227-1236.
6) Tsutsui H, Kayagaki N, Kuida K, Nakano H, Hayashi N, Takeda K, Matsui K, Kashiwamura S, Hada T, Akira S, Yagita H, Okamura H, Nakanishi K. Caspase-1-independent, Fas/Fas ligand-mediated IL-18 secretion from macrophages causes acute liver injury in mice. Immunity 1999; 11: 359-367.

7) Langrish CL, Chen Y, Blumenschein WM, Mattson J, Basham B, Sedgwick JD, McClanahan T, Kastelein RA, Cua DJ. IL-23 drives a pathogenic T cell population that induces autoimmune inflammation. J Exp Med 2005; 201: 233-240.

8) Martinez FO, Helming L, Gordon S. Alternative activation of macrophages: an immunologic functional perspective. Annu Rev Immunol 2009; 27: 451-483.

9) Saccani A, Schioppa T, Porta C, Biswas SK, Nebuloni M, Vago L, Bottazzi B, Colombo MP, Mantovani A, Sica A. p50 nuclear factor-kappaB overexpression in tumor-associated macrophages inhibits M1 inflammatory responses and antitumor resistance. Cancer Res 2006; 66: 11432-11440.

10) Singla DK, Singla RD, Abdelli LS, Glass C. Fibroblast growth factor-9 enhances M2 macrophage differentiation and attenuates adverse cardiac remodeling in the infarcted diabetic heart. PLoS One 2015; 10: e120739.

11) Sinha P, Clements VK, Ostrand-Rosenberg S. Reduction of myeloid-derived suppressor cells and induction of M1 macrophages facilitate the rejection of established metastatic disease. J Immunol 2005; 174: 636-645.

12) Mills CD. M1 and M2 Macrophages: oracles of health and disease. Crit Rev Immunol 2012; 32: 463-488.

13) Miro-Casas E, Covas MI, Farre M, Fito M, Ortuno J, Weinbrenner T, Roset P, de la Torre R. Hydroxytyrosol disposition in humans. Clin Chem 2003; 49: 945-952.

14) Soto-Alarcon SA, Ortiz M, Orellana P, Echeverria F, Bustamante A, Espinosa A, Illesca P, Gonzalez-Manan D, Valenzuela R, Videla LA. Docosahexaenoic acid and hydroxytyrosol co-administration fully prevents liver steatosis and related parameters in mice subjected to high-fat diet: a molecular approach. Biofactors 2019; 45: 930-943.

15) Dagla I, Benaki D, Baira E, Lemonakis N, Poudyal H, Brown L, Tsarbopoulos A, Skaltsounis AL, Mikros E, Gikas E. Alteration in the liver metabolome of rats with metabolic syndrome after treatment with hydroxytyrosol. A mass spectrometry and nuclear magnetic resonance - based metabolomics study. Talanta 2018; 178: 246-257.

16) Tome-Carneiro J, Crespo MC, Garcia-Calvo E, Luque-Garcia JL, Davalos A, Visioli F. Proteomic evaluation of mouse adipose tissue and liver following hydroxytyrosol supplementation. Food Chem Toxicol 2017; 107: 329-338.

17) Zhang L, Zhang J, Jiang X, Yang L, Zhang Q, Wang B, Cui L, Wang X. Hydroxytyrosol inhibits LPS-induced neuroinflammatory responses via suppression of TLR-4-mediated NF-kappaB P65 activation and ERK signaling pathway. Neuroscience 2019; 426: 189-200.

18) Utaipan T, Suksamrarn A, Kaemchantuek P, Chokchaisiri R, Stremmel W, Chamulitrat W, Chunglok W. Diterpenoid trigonoreidon B isolated from Trigonostemon reidioides alleviates inflammation in models of LPS-stimulated murine macrophages and inflammatory liver injury in mice. Biomed Pharmacother 2018; 101: 961-971.

19) Bloomer SA, Moyer ED, Brown KE, Kregel KC. Aging results in accumulation of M1 and M2 hepatic macrophages and a differential response to gadolinium chloride. Histochem Cell Biol 2020; 153: 37-48.

20) Wu BM, Liu JD, Li YH, Li J. Margatoxin mitigates CCl4induced hepatic fibrosis in mice via macrophage polarization, cytokine secretion and STAT signaling. Int J Mol Med 2020; 45: 103-114.

21) Wan J, Benkdane M, Teixeira-Clerc F, Bonnafous S, Louvet A, Lafdil F, Pecker F, Tran A, Gual P, Mallat A, Lotersztajn S, Pavoine C. M2 Kupffer cells promote M1 Kupffer cell apoptosis: a protective mechanism against alcoholic and nonalcoholic fatty liver disease. Hepatology 2014; 59: 130-142.

22) Silva S, Sepodes B, Rocha J, Direito R, Fernandes A, Brites D, Freitas M, Fernandes E, Bronze MR, Figueira ME. Protective effects of hydroxytyrosol-supplemented refined olive oil in animal models of acute inflammation and rheumatoid arthritis. J Nutr Biochem 2015; 26: 360-368.